

The formation of Mg-orthocarbonate through the reaction $\text{MgCO}_3 + \text{MgO} = \text{Mg}_2\text{CO}_4$ at Earth's lower mantle P – T conditions

Pavel N. Gavryushkin ^{*1,2}, Dinara N. Sagatova^{1,2}, Nursultan Sagatov¹, and Konstantin D. Litasov³

¹*Sobolev Institute of Geology and Mineralogy, Siberian Branch of Russian Academy of Sciences, prosp. acad. Koptiyuga 3, 630090 Novosibirsk, Russia*

²*Novosibirsk State University, Pirogova 2, Novosibirsk 630090, Russia*

³*Vereshchagin Institute for High Pressure Physics RAS, 108840, Troitsk, Moscow, Russian Federation*

Abstract

Orthocarbonates of alkaline-earth metals are the newly discovered class of compounds stabilized at high pressures. Orthocarbonates of Ca and Mg are the potential carbon host phases, transferring oxidized carbon in the Earth's lower mantle up to the core-mantle boundary. Here, we demonstrate the possibility for the formation of Mg_2CO_4 in the lower mantle at pressures above 50 GPa, by *ab initio* calculations. Mg_2CO_4 is formed by the reaction $\text{MgCO}_3 + \text{MgO} = \text{Mg}_2\text{CO}_4$, proceeding only at high-temperatures. At 50 GPa the reaction starts at 2200 K. The temperature decreases with pressure and drops down to 1085 K at the pressure of the Earth's core-mantle boundary, near 140 GPa. Two stable structures, Mg_2CO_4 -*Pnma* and Mg_2CO_4 -*P2₁/c*, were revealed. Mg_2CO_4 -*Pnma* is isostructural to Mg_2SiO_4 (forsterite) and stable below 80 GPa. Mg_2CO_4 -*P2₁/c* is isostructural to β - Ca_2SiO_4 (larnite) and stable above this pressure. Mg_2CO_4 -*Pnma* has a melting temperature of 16-18 % higher than the melting temperature of MgCO_3 (magnesite). At 23.7 GPa and 35.5 GPa, Mg_2CO_4 -*Pnma* melts at 2742 K and 2819 K, respectively. Acoustic wave velocities V_p and V_s of Mg_2CO_4 -*Pnma* are very similar to that of magnesite, while orthocarbonate owns stronger universal anisotropy in comparison with carbonate and has a larger coefficient A^U .

*Electronic address: gavryushkin@igm.nsc.ru, p.gavryushkin@ng.nsu.ru; Corresponding author

Introduction

During the recent decade, the crystal structure prediction technique became an integral part of high-pressure research. Numerous interesting experimental synthesis were guided by this technique, for instance, the synthesis of the high-pressure phases of alkaline carbonates Li_2CO_3 , Na_2CO_3 , and K_2CO_3 [?, ?, ?] and alkaline-earth carbonates CaCO_3 , MgCO_3 , and $\text{CaMg}(\text{CO}_3)_2$ [?, ?, ?, ?, ?, ?].

Orthocarbonates are another example for experimental confirmation of theoretically predicted structures. The possibility for the synthesis of alkaline orthocarbonates, the salts of the not yet experimentally observed orthocarbonic acid, has been suggested from the theoretical considerations [?, ?]. However, these predictions are still unverified by the experiment. The stability of the alkaline-earth orthocarbonates has not been considered till the last year. The performed crystal structure prediction in the $\text{MgO} - \text{CO}_2$ and $\text{CaO} - \text{CO}_2$ systems have revealed sp^3 -bonded structures with the intermediate stoichiometries, Ca_3CO_5 and CaC_2O_5 , stabilized at high pressures [?]. Thermodynamically stable structures of orthocarbonates with the Ca_2CO_4 or Mg_2CO_4 stoichiometry have not been revealed in these calculations.

Assuming the stochastic nature of the used methods of crystal structure prediction and possibility that some favorable structures can be missed in the calculation, we have performed a thorough search using both evolutionary algorithms (USPEX) and *ab initio* random methods (AIRSS) within the stoichiometry of orthocarbonate M_2CO_4 , where M is alkaline-earth metal, Mg, Ca, Sr, or Ba. As the result of this investigation, the structure $\text{Ca}_2\text{CO}_4\text{-}Pnma$ was obtained [?]. This structure lies above the energetic convex hull in the $\text{CaO} - \text{CO}_2$ system, i.e. it is stable relative to the decomposition on the known phases of this system, in particular to the mixture of $\text{CaO} + \text{CaCO}_3$. Further theoretical search has also shown that the similar structures of Sr and Ba orthocarbonates, $\text{Sr}_2\text{CO}_4\text{-}Pnma$ and $\text{Ba}_2\text{CO}_4\text{-}Pnma$, are also stable [?]. Recent experimental synthesis combined with single-crystal X-ray structure solution have confirmed the stability of the predicted $\text{Ca}_2\text{CO}_4\text{-}Pnma$ and $\text{Sr}_2\text{CO}_4\text{-}Pnma$ structures [?].

Undoubtedly, the most interesting orthocarbonate for the Earth sciences is the orthocarbonate of Mg. This compound can be readily formed within the slab subducted in the Earth's lower mantle from the locally abundant MgCO_3 and MgO by the simple reaction $\text{MgCO}_3 + \text{MgO} = \text{Mg}_2\text{CO}_4$. This reaction was speculatively suggested in [?] and even some calculations have been performed for the analysis of the possibility of its realisation [?]. However, due to the absence of the structure which would be more energetically favourable than the mixture of MgCO_3 and MgO , the possibility of the formation of Mg-orthocarboantes was not considered no theoretically, no experimentally. In the present study, using crystal structure prediction techniques, we performed the search of the structures in the composition Mg_2CO_4 and revealed such a structure, having stability field on the P-T phase diagram and the chance to be formed at the Earth's lower mantle P - T conditions.

Methods

To increase the chances for finding the energetically favorable structures we have used both USPEX and AIRSS methods, each of which has apparent advantages [?]. *Ab initio* structure prediction was complemented by the prediction technique based on the known structures of silicates and sulfates with isolated $[\text{SiO}_4]$ and $[\text{SO}_4]$ tetrahedrons. Mg_2CO_4 structures were produced from these structures by the corresponding replacement of the cations and consequent local optimizations. The following crystal structures have been used (numbers in parentheses indicate the number of formula units (f.u.) in the unit cell): Zn_2SiO_4 - $Fd\bar{3}m$ (8), Zn_2SiO_4 - $Imma$ (8), Zn_2SiO_4 - $Pbca$ (8), Zn_2SiO_4 - $Pnma$ (4), Zn_2SiO_4 - $I\bar{4}2d$ (4) [?], Mg_2SiO_4 - $Pnma$ (4) [?], Na_2SO_4 - $Fddd$ (8) [?], Li_2SO_4 - $P2_1/c$ (4) [?], and Ca_2CO_4 - $Pnma$ (4) [?].

The calculations with the USPEX method [?, ?, ?, ?] have been performed for 1-4 f.u. of Mg_2CO_4 at 25, 50, and 100 GPa. The seeding technique, implemented in version 10.2 of the USPEX, has been employed in all calculations. The aforementioned structures of silicates, sulfates, and orthocarbonate have been used as the seeds. Totally, around 3000 structures have been calculated at each pressure. Crystal structure prediction with AIRSS 0.9.1 [?, ?] has been performed only at 50 GPa for 2, 3, and 4 f.u. and a total of nearly 4000 structures have been generated in this calculation.

The energetic optimizations of the predicted structures have been performed within density functional theory (DFT), implemented in the VASP package [?, ?].

To take into account the temperature effect and calculate P - T phase diagram, we used the lattice dynamics method within the quasi-harmonic approximation (QHA). For this task, the lattice vibration frequencies were calculated with the PHONOPY code [?]. By our experience with P - T phase diagrams of carbonates, this technique reliably reproduces phase boundaries in the wide temperature range [?, ?, ?], up to 80-90 % of the melting temperature, if the process of dynamical disordering does not take place.

Melting temperatures of the predicted structures have been determined, using the so-called *Z-method*, based on the molecular dynamic (MD) simulations [?].

To determine the wave velocities V_p and V_s and assess anisotropy of Mg-orthocarbonates, static elastic stiffness tensor (C_{ij}) was calculated from the stress (σ)- strain (ϵ) relation $\sigma_i = C_{ij}\epsilon_j$. Based on these C_{ij} data, we calculated averages of bulk (B) and shear (G) moduli using the Voigt-Ruess-Hill scheme [?, ?]. Then we have determined compression (A_B), shear (A_G), and universal anisotropy (A^U) indexes.

The details of DFT, crystal structure predictions, thermodynamic and elastic property calculations, and MD simulations are given in *Supporting information*.

FindSym program [?] and instruments of Phonopy package have been used for the symmetry determination. VESTA and ToposPro [?, ?] programs have been used for the visualization of the crystal structures and figures preparation.

The topology of the structures was analysed with ToposPro and Robocrystallographer programs [?, ?].

1 Results and discussion

1.0.1 Predicted crystal structures and P–T phase idagram

In the crystal structure prediction calculations at 25 and 50 GPa, USPEX has revealed the Mg_2CO_4 - $Pnma$ structure as the most energetically favorable. This structure has lower enthalpy than Mg_2CO_4 - Cm , predicted by AIRSS, and structures, obtained based on the crystal structures of silicates and sulfates (Figure 1 and S1).

At 100 GPa, USPEX has found another favorable structure with monoclinic symmetry, Mg_2CO_4 - $P2_1/c$. The transition from Mg_2CO_4 - $Pnma$ to Mg_2CO_4 - $P2_1/c$ occurs at 52 GPa, and at higher pressures Mg_2CO_4 - $P2_1/c$ is the most energetically favorable among considered structures (Figure 1 and S1).

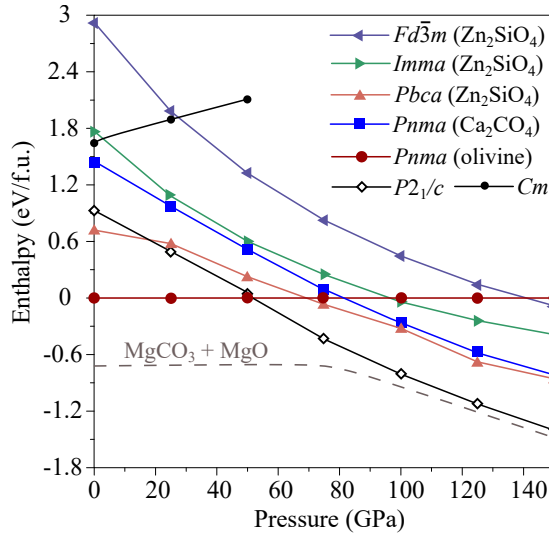


Figure 1: Enthalpy-pressure dependencies of Mg_2CO_4 structures. Isostructural compounds are indicated in brackets.

Revealed Mg_2CO_4 - $Pnma$ is isostructural to the mineral forsterite (Figure 2a,b). Atoms in both positions Mg1 and Mg2 are 6-coordinated, with the octahedral coordination polyhedron (Figure 2c). Mg_2CO_4 - $P2_1/c$ is isostructural to β - Ca_2SiO_4 (larnite) and can be considered as the monoclinic analogue of Ca_2CO_4 - $Pnma$. In crystal structure of Mg_2CO_4 - $P2_1/c$, there are two non-equivalent Mg sites. There is some ambiguity in determination of coordination numbers of Mg, due to the smooth variation of the bond distances. In the first site Mg(1) is bonded to six oxygen atoms, arranged in highly deformed

trigonal prism (Figure 2d), the Mg–O bond lengths within coordination polyhedron vary in the range 1.832–2.073 Å, while the seventh oxygen atoms is distant on 2.382 Å. In the second site, Mg(2) is bonded to eight oxygen atoms, forming relatively regular square antiprism, Mg–O distances vary in the range of 1.887–2.126 Å, the ninth atom is distant on 2.688 Å. For comparison, in $\text{Mg}_2\text{CO}_4\text{-}Pnma$ structure oxygen atoms in the first coordination sphere is distant on 1.815–1.888 Å for Mg(1) and on 1.781–1.95 Å — for (Mg2) site. All the presented bond lengths correspond to the pressure of 100 GPa. In both $Pnma$ and $P2_1/c$ crystal structures, coordination polyhedrons around Mg atoms share both vertices and edges with $[\text{CO}_4]$ tetrahedrons (Figure 2c,d). Transition from $\text{Mg}_2\text{CO}_4\text{-}Pnma$ to $\text{Mg}_2\text{CO}_4\text{-}P2_1/c$ is accompanied by the sufficient decrease of the volume equal to 5.7 % (Figure S2).

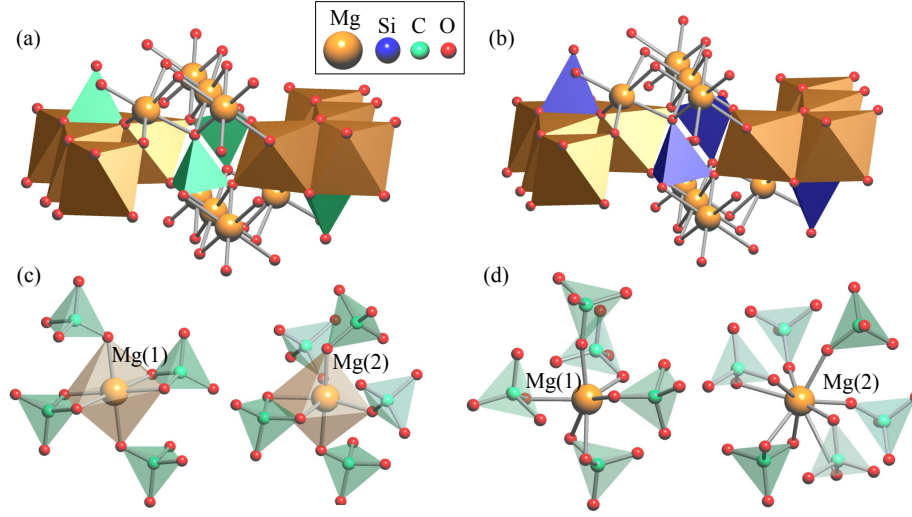


Figure 2: Comparison of crystal structures of $\text{Mg}_2\text{CO}_4\text{-}Pnma$ (a) and $\text{Mg}_2\text{SiO}_4\text{-}Pnma$ (b), coordination environment around Mg1 and Mg2 atoms in crystals structures $\text{Mg}_2\text{CO}_4\text{-}Pnma$ (c) and $\text{Mg}_2\text{CO}_4\text{-}P2_1/c$ (d).

Structural data for the $\text{Mg}_2\text{CO}_4\text{-}Pnma$ and $\text{Mg}_2\text{CO}_4\text{-}P2_1/c$ are given in the Table 2. Both structures are dynamically stable in the investigated pressure range 25–140 GPa, and there are no imaginary frequencies in their phonon dispersion curves (Figure 3, S3). In the *Supporting information*, we have also shown phonon dispersion curves of MgCO_3 and MgO (Figure S4) used for the construction of P – T phase diagram.

There is no analogy of the found transition from $\text{Mg}_2\text{CO}_4\text{-}Pnma$ to $\text{Mg}_2\text{CO}_4\text{-}P2_1/c$ in the Mg_2SiO_4 system. However, there is one in Ca_2SiO_4 system, where transformation of $\text{Mg}_2\text{CO}_4\text{-}Pnma$ into $\text{Mg}_2\text{CO}_4\text{-}P2_1/c$ corresponds to the transformation of $\gamma\text{-Ca}_2\text{SiO}_4$ into $\beta\text{-Ca}_2\text{SiO}_4$ with both transitions realized on compression [?]. Heating of $\beta\text{-Ca}_2\text{SiO}_4$ produces the phase $\text{Ca}_2\text{SiO}_4\text{-}\alpha'_H$ and similar

Table 1: Structural data of Mg_2CO_4 phases at 0 K.

P (GPa)	Space group	Lattice parameters (\AA , deg)			Atom	Coordinates		
						x	y	z
50	$Pnma$ (#62)	$a = 8.926$ $\alpha = 90.0$	$b = 5.565$ $\beta = 90.0$	$c = 4.221$ $\gamma = 90.0$	Mg1	0.000	0.000	0.500
					Mg2	0.721	0.250	0.531
					C1	-0.097	0.250	0.087
					O1	-0.091	0.250	0.770
					O2	0.548	0.250	0.284
					O3	0.169	0.552	0.786
100	$P2_1/c$ (#14)	$a = 4.408$ $\alpha = 90.0$	$b = 5.383$ $\beta = 117.65$	$c = 8.345$ $\gamma = 90.0$	Mg1	0.702	0.360	0.425
					Mg2	-0.022	0.000	0.693
					C1	0.355	0.282	0.082
					O1	0.146	0.334	0.638
					O2	0.681	0.245	0.197
					O3	0.272	0.168	-0.080
					O4	0.295	0.520	0.064

transition can be suggested for Mg_2CO_4 . In this case, on heating Mg_2CO_4 - $P2_1/c$ will be transformed into the new hypothetical phase Mg_2CO_4 - $Pnma$ -II similar to Ca_2SiO_4 - α'_H . The performed calculations of phonon dispersion curves of Mg_2CO_4 - $Pnma$ -II, produced based on the structure of Ca_2SiO_4 - α'_H by corresponding atomic replacements, have shown the dynamical instability of this phase (Figure S6). However, the stabilization of the structure by the factors, which are not considered within QHA can not be excluded.

The performed enthalpy calculations of the Mg_2CO_4 , MgO , and MgCO_3 structures have shown, that both Mg_2CO_4 - $Pnma$ and Mg_2CO_4 - $P2_1/c$ lie above the energetic convex hull, i.e. they are unstable and decompose to the mixture ($\text{MgO}+\text{MgCO}_3$) at 0 K (Figure S7).

However, performed calculations of the Gibbs free energies in the temperature range of 0–3000 K have shown that above some temperature Mg_2CO_4 became more energetically favorable than the ($\text{MgO}+\text{MgCO}_3$) mixture (Figure S8). At 20 GPa, this temperature is 2420 K, which is nearly equal to the melting temperature of MgCO_3 - $R\bar{3}c$ (magnesite) [?] (Figure 4). The pressure decreases the temperature of transition, and at 140 GPa Mg_2CO_4 - $P2_1/c$ can be synthesized from ($\text{MgO}+\text{MgCO}_3$) at temperatures higher than 1085 K. Thus, in the pressure range of 50–140 GPa, Mg_2CO_4 is formed at temperatures 250–1100 K higher than the corresponding temperatures of MgCO_3 melting (Figure 4). It suggests the possibility for the formation of Mg-orthocarbonate in most part of the Earth's lower mantle, at pressures higher than 50 GPa.

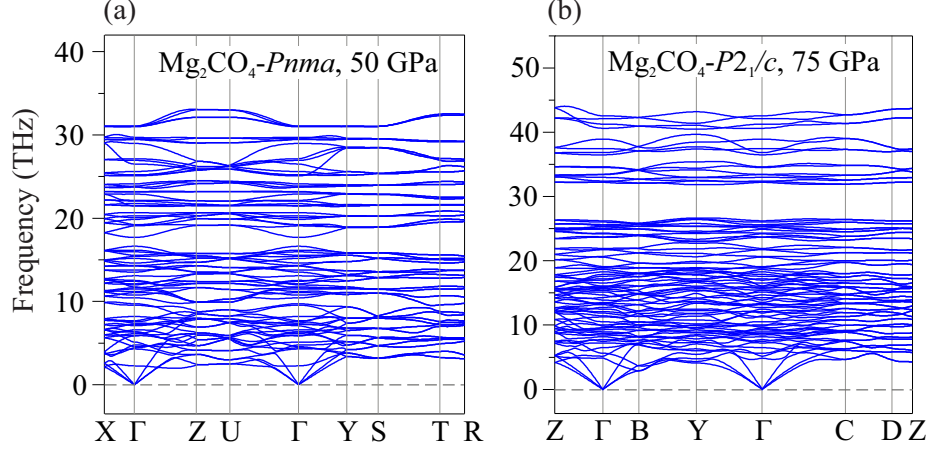


Figure 3: Phonon dispersion curves of $\text{Mg}_2\text{CO}_4\text{-Pnma}$ at 50 GPa (a) and $\text{Mg}_2\text{CO}_4\text{-P2}_1\text{/c}$ at 75 GPa (b).

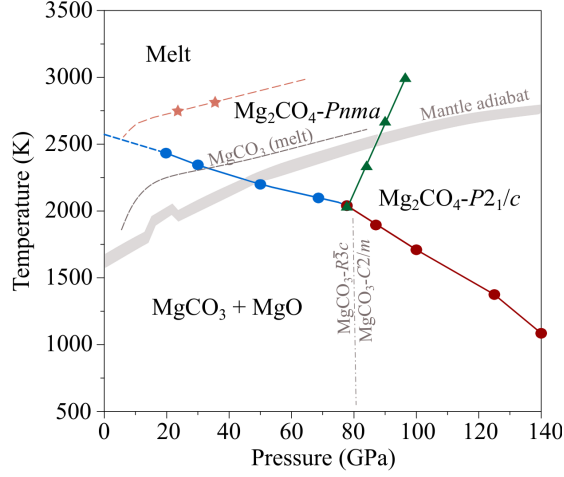


Figure 4: P - T phase diagram of Mg_2CO_4 . The asterisks represent calculated melting temperatures; the grey dash-dotted line — calculated phase transition boundary of MgCO_3 . The grey dashed line represent melting curve of MgCO_3 as reported by Solopova et al. [?]. Mantle adiabat is shown as grey solid line [?].

Raman spectra of the predicted phases

As Raman technique are now actively used for the identification of sp^3 bonded carbonates and orthocarbonates in high pressure experiments, we have calculated Raman spectra for the $\text{Mg}_2\text{CO}_4\text{-Pnma}$ [?, ?, ?].

The unit cells of $\text{Mg}_2\text{CO}_4\text{-Pnma}$ contain 28 atoms, i.e. there are 84 phonon

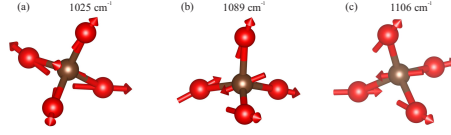


Figure 5: Displacement patterns in Raman modes of Mg₂CO₄-Pnma at 60 GPa. Arrows indicate the displacement of the atoms during the specific vibration.

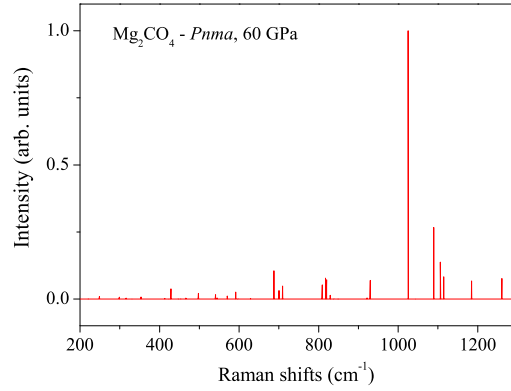


Figure 6: DFT-calculated Raman spectra of Mg₂CO₄-Pnma at 60 GPa.

modes. According to a group theoretical analysis, 36 Raman active modes are expected for Mg₂CO₄-Pnma: $\Gamma = 11A_g + 7B_{1g} + 11B_{2g} + 7B_{3g}$. The most intense mode (B_{2u}) corresponds to the bending and stretching vibrations in the [CO₄] groups and appears at 1025 cm⁻¹. The second (A_u) and third (B_{1g}) most intense modes appear at 1089 and 1106, correspondingly (Figure 5). The calculated Raman spectra at 60 GPa is shown in Figure ??.

Analysis of electronic density distribution

In both found structures, Pnma and $P2_1/c$, four C–O bonds within [CO₄] tetrahedron are of nearly the same length. At 100 GPa, in both *Pnma* and $P2_1/c$ structures these bond distances vary in the range 1.32–1.37 Å, which assume the covalent nature of all found bonds. The performed analysis of electron density distribution confirms this assumption. Accumulation of charge halfway along each of the four C–O bond, indicating on the covalent nature of all four C–O bonds within [CO₄] tetrahedron .

Melting temperature and seismic properties

To assess the effect of Mg-orthocarbonate formation on the melting of MgCO₃, we have estimated melting temperatures of Mg-orthocarbonate. The obtained

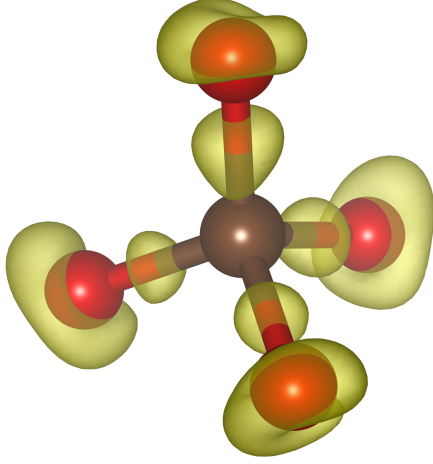


Figure 7: Isosurface of the electron density difference. The isosurface shows those regions in which the electron density is larger than that obtained by overlapping electron densities of non-interacting atoms.

Table 2: Bader charge analyses on Mg_2SiO_4 and Mg_2CO_4 at 0 GPa (in unit of e).

	Mg1	Mg2	C/Si	O1	O2	O3
Mg_2SiO_4	1.731	1.745	3.109	-1.645	-1.657	-1.641
Mg_2CO_4	1.724	1.745	1.914	-1.412	-1.340	-1.315

values of the Mg_2CO_4 - $Pnma$ melting temperatures at 23.7 GPa and at 35.5 GPa are 2742 K and 2819 K, respectively (Figure S9). These values are 16-18 % higher than the experimentally measured melting temperatures of magnesite and comparable with solidi of silicate rocks under lower mantle P-T conditions [?]. The melting curve of Mg_2CO_4 - $Pnma$ is nearly parallel to the melting curve of magnesite, with the difference in temperature being around 500 K.

To assess the effect of orthocarbonate formation on the seismic properties of carbonate, we have also calculated the elastic stiffness tensor and compressional/shear sound velocities (V_p/V_s) for Mg-carbonate and Mg-orthocarbonate. We have not aimed the investigation of trends for the changes of elastic properties on compression or their description during $Pnma \rightarrow P2_1/c$ transition, but only the rough comparison of carbonate and orthocarbonate properties. By this reason, calculations have been performed only at 50 GPa for Mg_2CO_4 - $Pnma$ and magnesite structures at 0 K.

The obtained elastic properties of Mg_2CO_4 and MgCO_3 are summarized in Table S1 and Table S2. Obtained values of C_{ij} , B , G , V_p , and V_s for magnesite are in good agreement with the previous results of theoretical calculations [?]. According to our results, the density and both bulk and shear moduli

of Mg_2CO_4 -*Pnma* are higher than that of magnesite by 4-5 %. Orthocarbonate is similar to carbonate in sense of seismic velocities V_p and V_s , but orthocarbonate is more anisotropic, owning higher universal anisotropy (A^U). The value of A^U for Mg_2CO_4 -*Pnma* is 0.4772, while that for magnesite is 0.2838.

Acknowledgments

This study was funded by the RFBR under research projects #20-03-00774 and #20-35-90043. Crystal structure prediction and calculation of P - T phase diagram were performed within the project #20-03-00774, while calculations of melting curve — within the project #20-35-90043. Calculations of elastic properties were supported by a state-assigned project of the IGM SB RAS.

The computations were performed using resources provided by the Novosibirsk State University Supercomputer Center.